SPE-171226-MS

Reservoir Monitoring of Hydrocarbon-Water Flood Front by Gravimetry Integrated within Reservoir Simulation

Gleb Dyatlov, Baker Hughes Inc.; Stig Lyngra, Alberto F. Marsala, and A.M. Ton Loermans (Now retired), SPE; Daniel T. Georgi, Saudi Aramco; Alexandr Vasilevskiy, Yuliy Dashevsky, and Carl M. Edwards, Baker Hughes Inc.

This paper was prepared for presentation at the SPE Russian Oil and Gas Exploration and Production Technical Conference and Exhibition held in Moscow, Russia, 14–16 October 2014.

Abstract

Gravimetry is a physical method with a large depth of investigation. Traditional applications include surface gravity observations for mining and oil exploration and borehole gravity logging for investigating formation bulk density.

A new application of gravimetry is large-scale reservoir saturation monitoring. Replacement of oil or gas by water leads to density changes in large volumes of the reservoir, which causes changes of the gravity field down hole as well as on the surface. Since borehole gravity sensors are closer to the reservoir than for surface acquired gravity data, borehole gravity data has better spatial resolution and are less affected by near surface changes.

This paper focuses on the problems of inversion of time-lapse gravity data for complex multilayered reservoirs and estimation of the accuracy of the reconstructed oil-water flood front. The traditional bitmap approach (dividing the reservoir into blocks) requires a huge number of parameters and leads to the well-known inversion ambiguity. This ambiguity can be reduced by introducing a priori information.

The basic idea of the presented approach is to obtain this a priori information by biasing the inversion with output from a history matched reservoir simulation data set. In this case, reservoir simulation saturation data from an onshore giant Middle Eastern oil field was used as input. By processing the simulation saturation data, it was possible to understand the behavior of the water saturation and oil-water flood front in the different layers of the reservoir. Using this knowledge, a 3D model of density changes was introduced. This model formed the basis of the optimization inversion algorithm used to fine-tune the actual location of the oil-water flood front on the basis of gravity data.

Numerical examples demonstrate how inversion and accuracy estimates work for data obtained from a realistic reservoir simulation. The proposed inversion technique will depict any differences from the history matched reservoir simulation saturation output and the gravity data; thus, the gravity data will allow enhanced precision of the reservoir simulation history match.

Introduction

Geology and reservoir engineering, the prodigious oil industry subsurface sciences, share the same paramount challenge of attempting to describe what occurs in the wide open spaces of the subsurface reservoir utilizing sparse well data (Dake 2001). As only a very small fraction of the subsurface can be observed directly or indirectly through cores, well logs and well production data, the in-between well reservoir characterization is more an art form than science. The dynamic changes between the wellbore control points can presently only be understood via matching the reservoir simulation models to re-produce the data acquired from the wells.

The Society of Petroleum Engineers (SPE) Research & Development (R&D) Committee outlined in the May 2011 issue of Journal of Petroleum Technology (JPT) the five grand R&D challenges facing the oil and gas industry (Judzis et al. 2011). One of the five challenges defined was higher resolution subsurface imaging of hydrocarbons. As part of the follow-up JPT article series covering each of the five grand challenges in depth, Neal and Krohn (2012) identified that the following technology options are the most advanced in offering a solution to the inter-well saturation mapping problem:

1. Seismic (3-D / 4-D seismic, surface, borehole and cross-well acquisition)
2. Electromagnetic (borehole to surface and crosswell)
3. Microgravity (borehole and surface acquisition)
4. Nano technology

This case study is based on a reservoir simulation data set that originates from an actual giant oil field located in the Eastern Province of Saudi Arabia. In a recent publication (Lyngra et al. 2013), it was concluded that in one of the producing reservoirs in this field, a heavily fracture dominated reservoir, an improved reservoir simulation model that can be fully utilized for well placement and oil production predictions can only be constructed by exploiting improved methods to identify fractures and reservoir saturations away from well control. To improve input for the described model and other complex models, seismic, electro-magnetic (Marsala et al. 2013) and microgravity (Loermans and Kelder 2006, Alshakhs et al. 2008) methods are all techniques currently being pursued by Saudi Aramco to improve inter-well fracture characterization and saturation mapping. Nano technology saturation mapping options have not been evaluated for this oil field in particular, but a new approach using magnetic nanomappers as a contrast agent for improving deep resolution for electromagnetic surveys (Al-Shehri et al. 2013) is currently being investigated in the research laboratory.

The results of successful field applications using surface microgravity surveys for gas/water reservoir monitoring are reported in several publications, e.g., Eiken et al. (2000), Brady et al. (2002), Brady et al. (2004), Bate (2005), Ferguson et al. (2007), Alnes et al. (2008), Brady et al. (2008) and AhmadZamri et al. (2009).

The potential of 4-D gravity surveys for inter-well oil/water reservoir surveillance has been evaluated based on modeling feasibility studies. Three of these case studies are using Saudi Arabian field data from as input for the microgravity sensitivity cases (Loermans and Kelder 2006, Alshakhs et al. 2008, Hadj-Sassi and Donadille 2010). In public domain technical literature, only two successful field applications for using microgravity data for monitoring of water enchroachment in oil fields are reported (Alawiyah et al. 2012, Hadi et al. 2013).

The Basic Principles of Microgravity

A gravitymeter measures the local acceleration of gravity (g, ~ 9.81 m/s^2) with a very high precision. Since the variations in g are caused by variations in the local mass distribution, adequate surface gravity measurements may help in the localization of large bodies with densities different from their surroundings, e.g., metal ore bodies and oil or gas fields. Prior the advancement of seismic technology, many oil and

gas fields were discovered aided by surface gravimetry. There are also some situations were seismic imaging is very difficult, like imaging close to large salt diapirs or below extensive salt layers (Van Nieuwenhuise and Pramik 2006), where surface gravitimetry is more practical.

The change of g with increasing depth in a well is profoundly influenced by the mass/density of the layers above the measuring point. This feature, the value of g being determined largely by the absolute position of the measuring point, can also be used as a method to establish true vertical depth (TVD) with an accuracy and precision no other method currently employed can match. A gravity tool measurement of g in a wellbore can be derived directly from Sir Isaac Newton's Inverse Square Law of Universal Gravitation (Newton, 1687). The physical principle of the borehole gravity measurement is illustrated in Fig. 1:

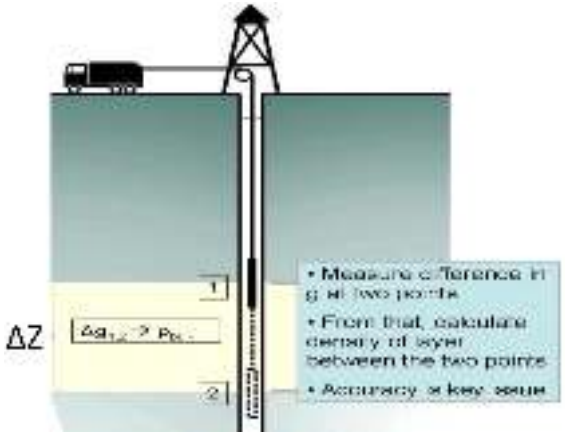

Figure 1—Principle of Borehole Gravity Measurements (after Chapin and Mann 1999, Loermans and Kelder 2006, Alshakhs et al. 2008)

As shown in Fig. 1, the Δg measurement of the strata away from the borehole is sensitive to the separation, ΔZ, between the two measurements. The bulk density (ρ_b, kg/m^3) of the slab of rock between the two points can be calculated utilizing the generalized equation (from Meyer, 2010):

$$\rho_b = \frac{f \quad \Delta g / \Delta Z}{4 \pi G}$$

In this equation, f is a gravity gradient correction term (1/s^2) and G is the Newton's Universal Gravitational Constant ~6.674 x 10^{-11} m^3/kg s^2.

By increasing ΔZ in the measurement, more rock is affecting Δg; hence, the further away from the wellbore reservoir effects can be detected. The Δg can be a result of stratigraphic, structural, or diagenetic effects (matrix or porosity effects). However, the more substantial Δg effects are caused predominantly due to the existence of different reservoir fluids, i.e., oil, water, and/or gas. The following general formula describes the total bulk density:

$$\rho_b = (1-\varphi)\rho_{matrix} + \varphi(\rho_{wat} S_{wat} + \rho_{oil} S_{oil} + \rho_{gas} S_{gas})$$

where: φ is the porosity, S is the water / oil / gas saturations and ρ is the density of the fluids and matrix.

In a case with water influx into a gas zone with water substituting gas, the difference in Δg and ρ_b can be substantial due to the much larger water density as compared to gas density. The current surface gravimeter tools have a precision of less than 5 μGal (Alawiyah 2012). For reference, the absolute value of g is ~ 9.8 x 10^8 μGal. AhmadZamri et al. (2009) reports from monitoring of injected waste gas into an aquifer at ~ 5000 ft depth that surface gravity anomalies of ~20 μGal were initially observed around the injector wells. These anomalies continued to grow in strength and size with increasing cumulative injected gas volume, as observed by five time lapse surface surveys. The ultimate precision was reported to vary from survey to survey, but the stated average precision was less than 6 μGal.

For the oil field water flooding or water encroachment case, however, the small bulk density changes associated with fluid substitution produce a very small change in the gravity field. This is directly related to the much smaller density difference between oil and water than for the gas/water case. A gravity tool with a very high precision will be required to capture these slight Δg changes. In the Alshakhs et al. (2008) case study, a synthetic surface microgravity data set was generated using reservoir simulation saturation output. Based on inversion of this synthetic microgravity data, it was concluded that a tool precision of ~0.01 μGal is required to be able to successfully detect inter-well fluid substitution changes. Thus, a

gravitymeter tool precision improvement of almost three orders of magnitude is a prerequisite for successful microgravity water encroachment monitoring.

Microgravity: State-of-the-Art and R&D Technology Challenges

The borehole gravity theory was described in the previous section to illustrate the simple relationships between Δg and the reservoir fluid saturations. The following gravity modeling sections assume interpretation of 4D time lapse microgravity surveys covering the reservoir area of interest.

Time-lapse refers to two (or more) gravity-monitoring surveys measured at different calendar times over the same area. The difference is taken between the monitoring survey and the original (base) survey. The most successful result will occur if a base survey is performed prior to water injection or aquifer influx takes place with the reservoir at its original oil saturation state. The time lapse signal eradicates the gravitational influence of all the above reservoir geological complexities and eliminates reservoir heterogeneity effects since it captures the changes in the gravity signal due to water encroachment alone.

The two successful Indonesian oil field applications (Alawiyah et al. 2012, Hadi et al. 2013) were based on interpretations of time lapse surface microgravity surveys. In these two publications, time lapse microgravity anomalies were used for a qualitative assessment of water injection encroachment without any attempt to quantify time lapse water saturation changes. This is likely due to microgravity tool precision. Thus, these two data sets would only be meaningful as time lapse and tied to other original saturation state calibration data.

A similar technique was used for the Prudhoe Bay gas cap water injection project (Brady et al. 2004, Brady et al. 2008) where time lapse surface microgravity measurements where superimposed to identify areas of water encroachment. The base line survey results were also published (Brady et al. 2002, Brown et al. 2002). Also in this Alaska field application, no maps quantifying saturation changes have been included in any of the many publications dealing with this project.

It should be noted that the time expended from the feasibility modelling publications, for both the Indonesian oil field applications (Santoso 2004) and the Prudhoe Bay case (Brady et al. 1993, Brady et al. 1995, Hare et al. 1999), until publication of time lapse interpretation results is in order of 8-9 years, which illustrates that these type of surveys take careful planning and execution for successful results. The author lists for both the Alaska and the Indonesian projects illustrate the technical complexities with the involvement of operating companies, universities, research institutions and service providers in both the planning and interpretation phase.

For a successful implementation of microgravity for oil field water encroachment monitoring and inter-well saturation quantification, the designed monitoring program will require time lapse surface microgravity surveys integrated with borehole surveys. The borehole gravity measurements will improve the accuracy of the fluid saturation gravity inversion since the measured Δg is a result of reservoir effects alone and much higher signal amplitude will be detected. Moreover, significant understanding of the area around each well can be obtained by gradually increasing the ΔZ; thus, increase the radius of investigation away from the wellbore to accurately identify the location of the flood front. This information can be used to calibrate a surface gravity data set run in close time proximity, which may in turn resolve some of the issues related to non-unique inversion of gravity data into hydrocarbon saturation.

The current generation borehole gravity tool has been available for decades, but the existing tool diameter is typically above 4 inches (Loermans and Kelder 2006), dependent on pressure and temperature ratings. The existing mass-spring gravity tool technology also requires the surveyed well to be less than 14° deviation from vertical (Chapin and Mann 1999). Ander and Biegert (2006) estimated that less than 0.5% of the wells in the world can be successfully surveyed by borehole gravity measurement through the target reservoir interval due to this tool size and inclination limitations. Moreover, an improvement in borehole tool precision is required to be able to use the borehole gravity measurements for saturation inversion.

The gravity technology shows significant promise, but the prerequisite R&D developments to develop a borehole tool of appropriate size with significantly improved gravity sensor accuracy (Brady et al. 1993, Loermans and Kelder 2006, Meyer 2010) are yet to be delivered, which pose a significant limitation for present day application of gravity technology. The improvement in the tool precision is feasible by construction of new generation gravity tools. One of the possible options for tool development with the required precision is to build an Atom-Interferometry gravity tool (Peters et al. 1997, Alshakhs et al. 2008).

Microgravity was mentioned as one of four contenders to resolve the inter-well saturation mapping challenge, as presented by Neal and Krohn (2012), as part of the five grand R&D challenges facing the oil and gas industry (Judzis et al. 2011). For microgravity to be a serious alternative for inter-well saturation mapping for oil fields under waterflood, the borehole gravity measurement hardware development needs to be given significant R&D priority.

Non-uniqueness for Microgravity Survey Hydrocarbon Saturation Inversion

Gravity is a potential field, which makes inversion of gravity data intrinsically non-unique (Zhdanov 2002, Tarantola 2005, Hadj-Sassi and Donadille 2010). The reason for the inversion non-uniqueness is due to that there are many density (i.e. saturation) distributions that generate the same potential field, and; hence, the same microgravity response. Hadj-Sassi and Donadille (2010) reviews the many technical publications that provide different alternatives for reducing the non-uniqueness of the hydrocarbon saturation gravity survey inversion. Jackson (1979) discussed the use of a priori information to resolve the non-uniqueness. Glegola et al. (2012) report in two journal articles the use of reservoir simulation to improve the quality of inversion of surface gravity data for monitoring of water influx into a gas reservoir.

In this paper, the approach utilized was to obtain a priori information by biasing the gravity inversion with output from a history matched reservoir simulation data set. By processing the gravity results using the simulation saturation data as a starting point, it was possible to understand the behavior of the water saturation and oil-water flood front in the different layers of the reservoir. Using this knowledge, a 3D model of density changes was introduced. This model formed the basis of the optimization inversion algorithm used to fine-tune the actual location of the oil-water flood front on the basis of gravity data.

Numerical examples demonstrate how inversion and accuracy estimates work for the data obtained from a realistic reservoir simulation data set. The proposed inversion technique will depict any differences from the history matched reservoir simulation saturation output and the gravity data; thus, the gravity data will allow enhanced precision of the reservoir simulation history match.

Background for Middle East Field Case for Gravity Monitoring of Large-scale Hydrocarbon Water Fronts

The key issues raised for a particular gravity monitoring case are: (1) the level of gravity field changes, and (2) the possibility of recovery of the oil-water contact (OWC) with reasonable accuracy from practically available measurements (inversion and resolution analysis). The answer to the first question can be obtained simply by forward gravity modeling based on the saturation output. The second question is more complicated, since inversion of gravity data is known to be ambiguous, unstable and non-unique. This is particularly true when inverting a surface gravity data set with sparse or no available borehole data. If inversion of gravity data uses a priori information for the sought solution, the quality of the result (and often the speed of the inversion) depends strongly on how fully the available field data is used to steer the solution and also eliminate impossible cases.

Some a priori factors to consider for this field case are: (1) large reservoir thickness, (2) large number of different reservoir layers, and (3) peripheral water flood. Thus, the water saturation changes gradually over a large area along the water flood direction and the OWC surface extends over a substantial distance

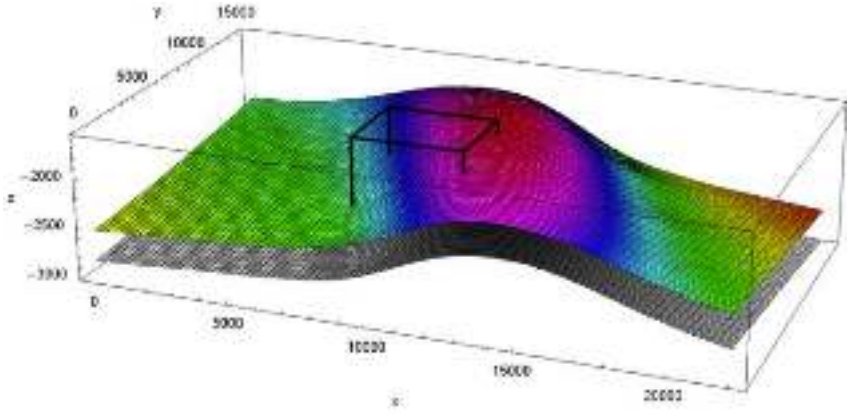

Figure 2—The Reservoir Section Utilized in the Simulation

in the horizontal direction, as discussed below in the Description of Field, Reservoir and Reservoir Simulation Data Set section. Due to these a priori factors, the traditional gravimetry approach where the volume is partitioned into blocks (of constant density) has several disadvantages: (1) a large number of blocks are needed to approximate the density changes, (2) it is difficult to describe the fact that the sought density changes result from the OWC movement, and (3) there is no straightforward means to translate block densities into the OWC location.

In this case, a different approach was used for the inversion in which the density changes are described through the OWC location and necessary a priori information is taken from a reservoir simulation. The advantages of this method are (1) that the a priori information is used already in the model of sought density changes, (2) the inversion gives immediately the OWC location, and (3) a reasonable result can be obtained even from measurements in a few boreholes.

In the microgravity modeling in this field case, a priori information was introduced assuming the density changes $\rho^{diff}(r)$ at a grid cell location $r = (x, y, z)$ during a given time interval $[t_1, t_2]$ are connected with the water saturation changes $S^{diff}(r) = S(r, t_2) - S(r, t_1)$ by the formula $\rho^{diff}(r) = \phi(r)(\rho_{water} - \rho_{oil})S^{diff}(r)$, where $\phi(r)$ is the porosity and ρ_{water} and ρ_{oil} are the water and oil densities. In this case, water and oil densities of 1.06 g/cm^{3}and 0.85 g/cm^3, respectively, were used as input. A gravity field change is defined by the vertical component $g_z^{diff}(r)$ of the gravity field measured at sensor points in a borehole:

$$g_z^{diff}(r) = \gamma \int_V \rho^{diff}(r') \frac{z - z'}{|r - r'|^3} dV(r'),$$

where V is the volume of the part of the reservoir where the density changes occurs.

Description of Field, Reservoir and Reservoir Simulation Data Set

In this paper, a realistic simulation of a giant Middle Eastern oil field is used for a surface microgravity sensitivity study. The oil field composed of two main naturally fractured carbonate reservoirs (Lyngra et al. 2013, Marsala et al. 2013), separated by a thick non-permeable zone. The Upper reservoir is prolific, while the Lower reservoir is relatively tight and highly fractured. The reservoir pressure data from the early production period confirmed communication between the two reservoirs through several large scale fractures crossing the non-permeable zone. In the Lower reservoir, well log observations show a variable oil/water distribution. No direct measurements of fluid saturations are available in the inter-well areas. Both reservoirs have been under peripheral water flood during most of the production period.

The entire reservoir used in simulation is shown in Fig. 2. The reservoir is divided into 36 layers. A simulation history match and prediction was carried out for an 86 year time period. A summary output time step of 1 year was used to determine the water saturation in each grid cell. The simulation data set

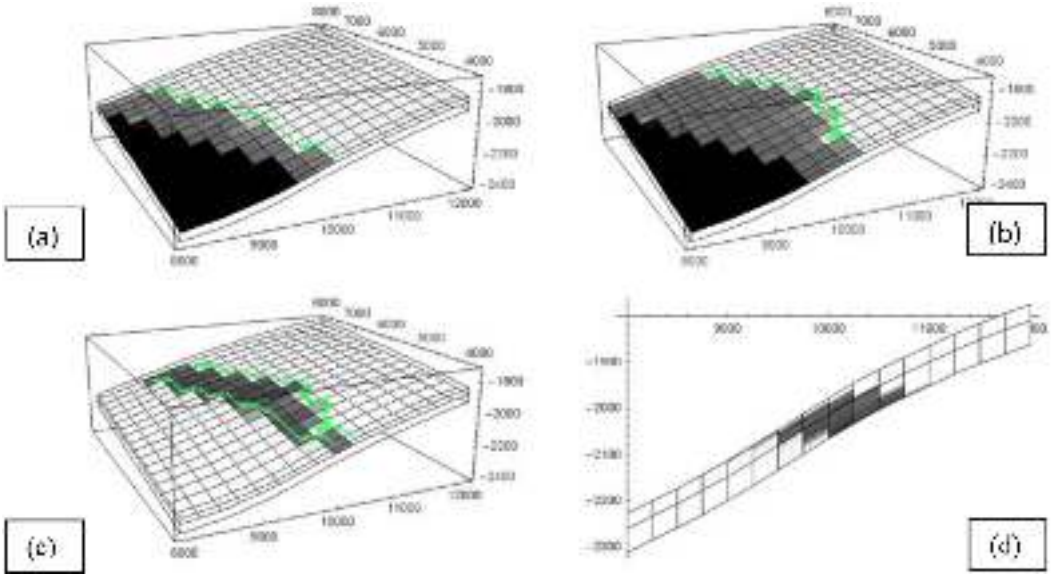

Figure 3—Examples of Water Saturation and Water Saturation Changes in Model Layer 18

shows that the fluid movement occurs mainly in the Upper reservoir (layers 1–26), which is consistent field performance and reservoir description.

The cube in Fig. 2 shows the area that was used for forward and inverse gravity modeling. The gravity modeling was done for the years 25-30 and limited to only the top 26 layers (Upper reservoir). Fig. 3 offers some examples of the model water saturation and water flooding saturation changes over time. The upper left panel (Fig. 3a) displays the water saturation in year 25 in model layer 18. For comparison, the year 30 water saturation in the same layer is the upper right panel (Fig. 3b). The water saturation changes from years 25 to 30 in the lower left panel (Fig. 3c) clearly demonstrate the flood front movement in layer 18 over the five year period. The lower right graphic (Fig. 3d) shows the water saturation changes in same area in cross-sectional view. The green lines are OWC lines where the saturation (oil or water) equals 15%.

Reservoir Model Simulation Analyses

As mentioned in the section Background for Middle East Field Case for Gravity Monitoring of Large-scale Hydrocarbon Water Fronts adequate bitmap description of the density changes caused by the OWC propagation would require enormously many blocks and would complicate the inversion and location of the OWC line. Our approach is to reduce the number of unknowns and describe the sought density changes by a model which includes

1. OWC line in each reservoir layer;
2. the water saturation profile in each layer as a function of the distance to the OWC line.

We keep the OWC line as the only sought parameter determined through inversion of the gravity data, while the water saturation profile is the a priori information extracted from the reservoir simulation.

This basic idea needs two amendments. First, in view of the large reservoir thickness and different properties of layers, each layer has its own OWC line, namely the OWC line in the lower layers is ahead of that in the upper layers. In our model we seek for the OWC line in one (reference) layer only. The distances between the OWC lines in the other layers and that in the reference layer are supposed to be given a priori and determined like the saturation profiles from the reservoir simulation. Second, we deal with the changes in the time interval $[t_1, t_2]$ rather than the absolute values at a particular time. It means that either both OWC lines at t_1 and t_2 are sought or one of them (naturally, the one at t_1) is given. Also,

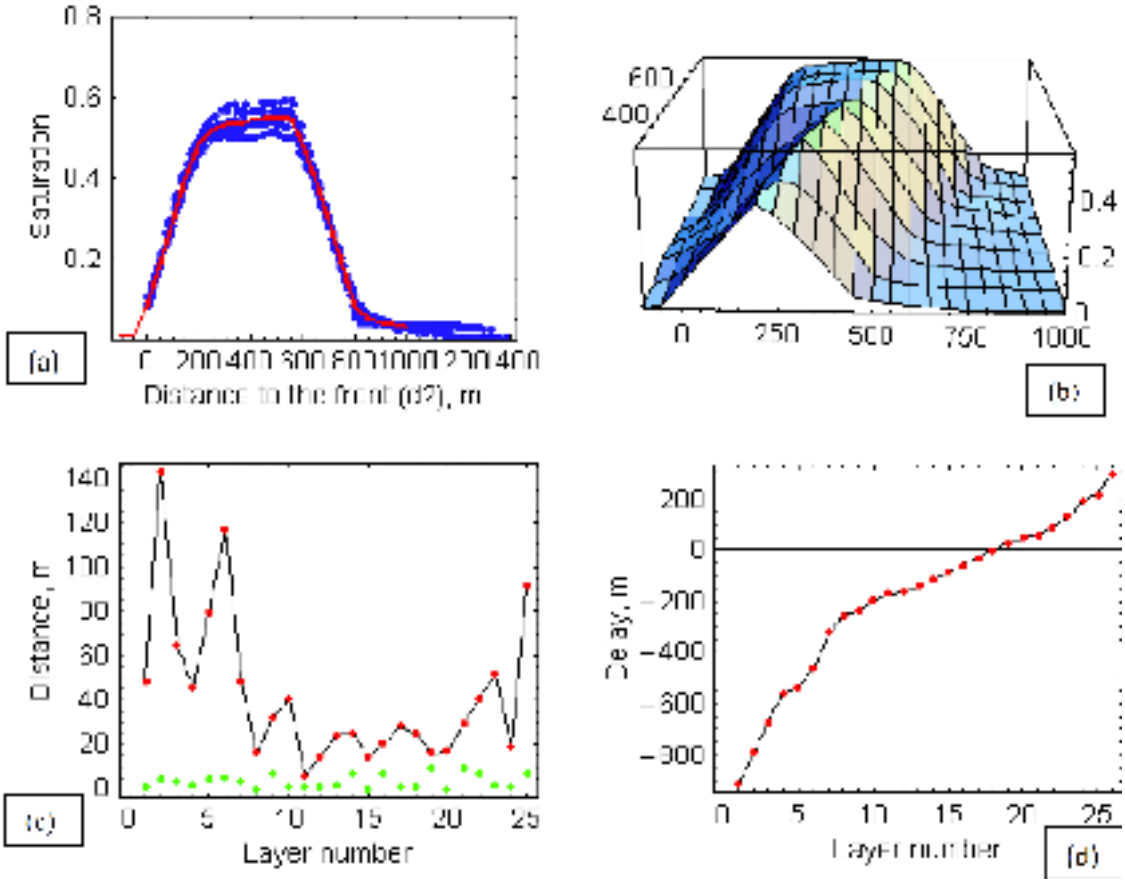

Figure 4—Reservoir Simulation Saturation Output Analyses

from the reservoir simulation we actually extract the profile of water saturation changes rather that the saturation itself.

Analysis of the reservoir simulation and extraction of the a priori information goes as follows. Fix t_1 and t_2 and consider the area of the reservoir where the density changes happen. For each t_i, $i = 1, 2$, in every layer k draw the line on which the water saturation equals some small value (15% is assumed). This is the true OWC line $\gamma_k(t_i)$. For the neighboring layeres k and $k + 1$ we find the average distance between $\gamma_k(t_i)$ and $\gamma_{k+1}(t_i)$ and use it as a priori information as stated above.

To find the profile of water saturation changes in the k th layer, we pick up randomly a large number of points between $\gamma_k(t_1)$ and $\gamma_k(t_2)$ and plot the water saturation versus the distance from the point to the OWC lines. The plot clearly reveals the sought dependence (see Fig. 4a).

Other approaches to reduction of the number of unknowns are proposed by Davis et al. (2008), Krahenbuhl and Li (2008), and Krahenbuhl et al. (2010).

In the next section we provided a detail definition of the model density changes that provides a basis for inversion.

Definition of the Model Density Changes

Each grid cell is designated by $r = (x, y, z)$. It is assumed that the water saturation is homogeneous in the vertical direction within each layer and, hence, depends on the x, y-coordinate and the layer number k, $S(r, t) = S_k(x, y, t)$. For each layer k and time (t), the OWC line (γ) is introduced:

$$\gamma_k(t) = \{(x, y) \mid S_k(x, y, t) = S_0\}$$

based on the cell oil saturation S_0 equals some low value (15% is assumed). The reporting times t_1 and t_2 are selected and for each layer number k, the saturation changes are evaluated:

$$S_k^{diff}(x,y) = S_k(x,y,t_2) - S_k(x,y,t_1).$$

The green lines in Fig. 3 show the OWC lines at reporting times t_1 and t_2, $\gamma_k(t_1)$ and $\gamma_k(t_2)$. For a given point (x, y), $d_i(x, y)$, is defined to be the distance from (x, y) to $\gamma_k(t_i)$ and $w(x, y) = d_1(x, y) + d_2(x, y)$ is the local width of the area of density changes. This analysis shows that the saturation depends mainly on $d_2(x, y)$ and $w(x, y)$. In Fig. 4a, the saturation changes are shown versus $d_2(x, y)$ for a large number of random points between $\gamma_k(t_1)$ and $\gamma_k(t_2)$ for $w(x, y)$ close to 600m. Thus, from the reservoir simulation, the approximate statistical dependence of the saturation changes $\overline{S}_k(d_2, w)$ is obtained such that $S_k^{diff}(x, y)$ is approximated well by $\overline{S}_k(d_2(x, y), w(x, y))$. The red line in Fig. 4a describes the average saturation changes. The 2D plot in Fig. 4b shows the average saturation changes as a function of d_2 and $w = d_1 + d_2$.

If the connection between front lines $\gamma_k(t)$ in different layers at a fixed time (t) is considered, it is observed that the OWC lines in lower layers are moving ahead of the flood front in the upper layers (see cross-section, Fig. 3d). The average distance between $\gamma_k(t)$ and $\gamma_{k+1}(t)$ is defined as $\overline{\delta}_k$. Analysis of the simulation results show that the distance measured at different points along the OWC lines does not differ much from the average values $\overline{\delta}_k$ (as displayed in Fig. 4c). Fig. 4c displays the mean distance $\overline{\delta}_k$ between the OWC lines in neighboring layers (red) and the mean square deviation from $\overline{\delta}_k$ (green).

We introduce the values (see Fig. 4d): $\overline{\Delta}_1 = 0$, $\overline{\Delta}_k = \overline{\delta}_1 + \cdots + \overline{\delta}_{k-1}$, $k > 1$, $\Delta_{k,k_0} = \Delta_{k,1} - \Delta_{k_0,1}$,

where k_0 is the number of an assumed reference layer. Consequently, the OWC line $\gamma_k(t)$ is ahead of $\gamma_{k0}(t)$ by the distance $\overline{\Delta}_{k,k_0}$ (this distance is negative if $k < k_0$). From Fig. 4d, it is evident that the OWC crossing the full Upper reservoir section (layers 1-26) extends for ~1000m laterally at any given point in time. Fig. 4d presents the distance $\overline{\Delta}_{18,k}$ from the OWC lines to that in the 18th (reference) layer.

The mean saturation changes $\overline{S}_k(d_2, w)$ and distances $\overline{\Delta}_{k,k_0}$ are used in constructing a model of density changes for gravity modeling purposes.

A reference layer k_0 is chosen and $\gamma_{k_0}^1$ and $\gamma_{k_0}^2$ are the sought OWC lines at t_1 and t_2 in the reference layer. Using the a priori information determined above, the model density changes are defined as:

$$\rho^{model}(r;\gamma_{k_0}^1,\gamma_{k_0}^2) = \varphi(r)(\rho_{water} - \rho_{oil})\overline{S}_k(d_2 - \overline{\Delta}_{k,k_0}, d_1 + d_2),$$

where k is the number of the layer containing the point $r = (x, y, z)$ and d_i is the distance from (x, y) to $\gamma_{k_0}^i$. The meaning of this formula is that, for a given point $r = (x, y, z)$ within the reservoir, we determine the number k of the layer which contains this point and the distances d_1 and d_2 to the sought OWC lines $\gamma_{k_0}^1$ and $\gamma_{k_0}^2$ in the reference layer k_0. Then we take the distance $d_2 - \overline{\Delta}_{k,k_0}$ from r to the OWC line in the k th layer (which is ahead of that in the k_0 th layer for $k > k_0$ and behind for $k < k_0$) and the local width $d_1 + d_2$ of the saturation changes zone. Finally, the model saturation change $\overline{S}_k$ is multiplied by the density contrast and porosity. It is worth to note that the unknowns are only the OWC lines $\gamma_{k_0}^1$ and $\gamma_{k_0}^2$, while the other parameters are a priori information obtained from the reservoir simulation. The flood front lines are defined by interpolation using 500m spacing between simulation output points.

Inversion

Once the model density changes $\rho^{model}(r;\gamma_{k_0}^1,\gamma_{k_0}^2)$ are introduced, the model gravity changes are calculated by the formula:

$$g_z^{model}(r;\gamma_1,\gamma_2) = G\int \frac{\rho^{model}(r';\gamma_{k_0}^1,\gamma_{k_0}^2)(z - z')}{|r - r'|^3} dV(r')$$

where the integral is calculated by the Monte-Carlo method. The inversion minimizes the function:

$$R(\gamma_{k_1}^1,\gamma_{k_2}^2)=\left(\frac{1}{S}\sum_{s=1}^{S}\left|g_s^{model}(r_s;\gamma_{k_1}^1,\gamma_{k_2}^2)-g_s^{meas}(r_s)\right|^2\right)^{1/2},$$

where S is the number of sensor points r_s and $g_s^{meas}(r_s)$ are the measured gravity field changes. The true changes were calculated directly from the reservoir model plus random error. The minimization is carried out by the steepest descent method.

Inversion of Synthetic Data

As described in the Description of Field, Reservoir and Reservoir Simulation Data section, the Upper reservoir (layers 1-26) simulated saturations in the region shown as a cube in Fig. 2 were used for forward and inverse gravity modeling of the time period 25-30 years. Fig. 5a shows nine pseudo measurement boreholes located with 500m spacing. The measurements are made along the boreholes with 10m increments from 100m below to 400m above the top reservoir. The bottom panel (Fig. 5b) shows the gravity field changes in the colored boreholes. The color of the gravity changes and color coded borehole location are the same. The signal in the borehole close to the OWC line reaches 20 μGal at the top reservoir.

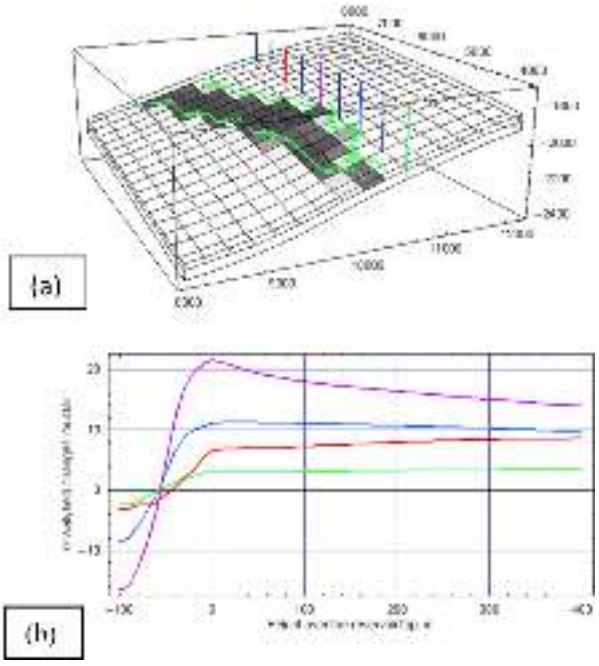

Figure 5—Gravity Field Changes in Boreholes

In the boreholes close to the OWC, the gravity field changes reach 10-20 μGal. It should be noted that the plots show much larger variation within the reservoir (-100 m to 0 m) than above its top (0 m to 400 m). This illustrates that the borehole gravity measurement data acquired within the reservoir near the OWC are more sensitive to the sought density changes than those further away. For the inversion, the computed gravity field changes are contaminated with 5 μGal noise.

Fig. 6 shows the gravity field changes at three different depths: (a) on the surface, (b) 500m above top reservoir and (c) top reservoir depth. It is clear that for the top reservoir case, the changes are much more substantial than for the two other cases. Moreover, the gravity field changes downhole better reflect the density changes caused by the OWC movement. This clearly demonstrates the advantages of borehole data over surface data for monitoring of OWC movements.

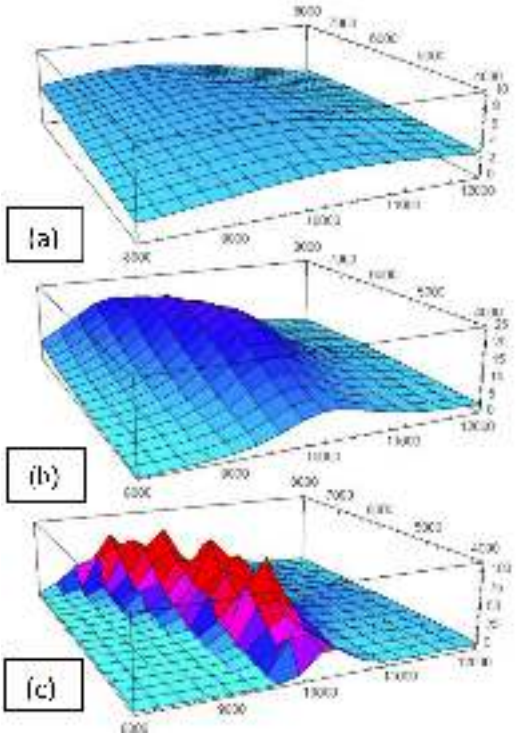

Figure 6—Gravity field changes at different depths: on surface (upper panel), 500m above the reservoir top (middle panel), and on top reservoir (lower panel).

The corresponding maximum values for the surface, 500m above the top reservoir and on top reservoir are 6, 23, and 108 μGal, respectively. The changes in the bottom Fig., Fig. 6c, reflect well the structure

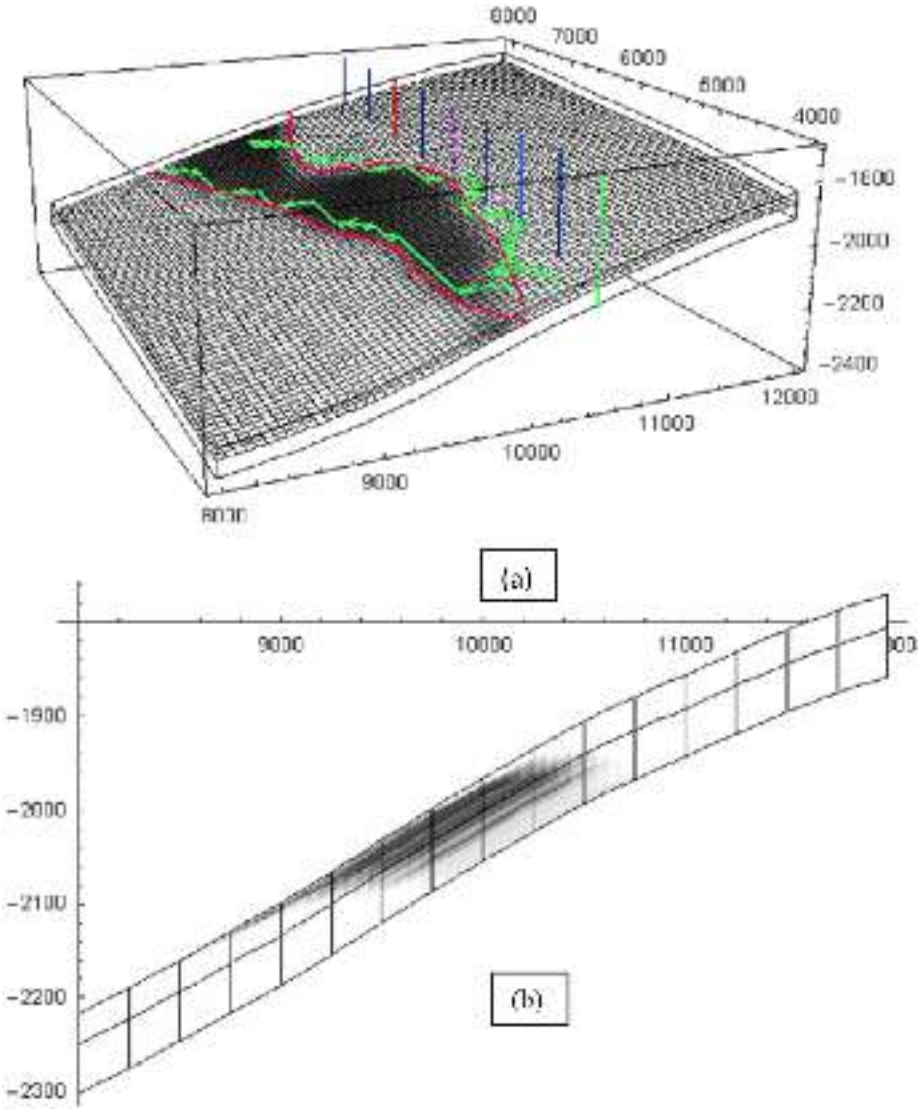

Figure 7—Density Changes Obtained by Inversion of the Simulated Gravity Data.

of the density changes caused by the OWC movement, while the surface data is oversmoothed and lacks resolution.

For the inversion, the unknown OWC line is parameterized by 9 points with spacing 500m (the same as for boreholes). The actual profiles of saturation changes and distances were obtained from the reservoir simulation (Fig. 4b and Fig. 4d). The reference layer is the 18th layer. The initial guess is the straight line 500m apart from the line of boreholes. The black and white density plot, shown in Fig. 7a, displays the density changes from inversion in the 18th layer. The red lines are the model OWC lines at t_1 and t_2. The green lines are the true OWC lines, as output from the simulation model. The fit is equal to 7.2 μGal. The accuracy depends on the distance from the OWC line to the measurement boreholes.

A good agreement is observed near the measurement boreholes in the central section. For most locations the gravity inverted OWC lies within 50-100m from the true front. The greatest deviation is 170m (near the blue borehole). In the upper part (towards y=8000), where the boreholes are located more than 500m from the WOC line, the inversion is poor. The poorer reconstruction at the bottom section (towards y=4000) is explained by the small width of the density change area and proximity to the modeling region boundary. Fig. 7b presents the density changes in a cross-section located at y=6000m.

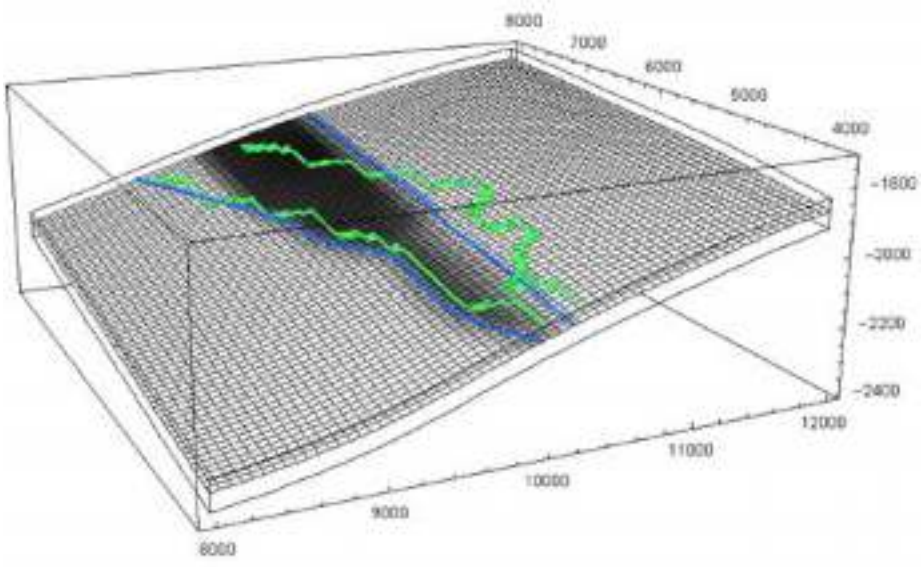

Figure 8—Density Changes Obtained from the Surface Gravity Data Only

The proposed algorithm was also applied to inversion of surface gravity data alone using 500m Cartesian grid. The resulting OWC (see Fig. 8 blue lines) is slightly different from the initial guess (the straight line $x=10000$m). At the same time, residual model gravity fit is 0.2μGal which is significantly less than the precision of the existing technology surface measurements, as discussed in The Basic Principles of Microgravity section, but higher than the tool precision of ~0.01 μGal recommended by Alshakhs et al. as the required tool precision to allow a successful inversion of surface gravity data. However, for some locations, the resulting OWC is distant from the true OWC by more than 500m. This illustrates that for this example, the uncertainty of the inversion for the location of the OWC from surface data alone is more than 500m.

Conclusions

Using a priori information is crucial for the quality of inversion of gravity data. In reservoir monitoring, the a priori information can be obtained from reservoir simulation output, once the geometry of the reservoir, properties of the layers, and the flooding regime are known. An algorithm is shown to illustrate how to extract and use this information to reduce the number of unknowns and guide the inversion towards likely outcomes and eliminate impossible scenarios.

This inversion of simulated time-lapse gravity data demonstrates the potential of the 4D gravity measurements. For the modeled field used, a typical Middle Eastern giant reservoir, the added value of using borehole gravity data rather than surface gravity data is obvious from the much better defined position of the calculated (inverted) OWC. For microgravity to be a serious alternative for inter-well saturation mapping for oil fields under waterflood, the borehole gravity measurement hardware development needs to be given significant R&D priority.

Acknowledgements

The authors thank Saudi Aramco for providing the reservoir simulation data set used for the microgravity forward modeling and inversion analysis. We also thank Baker Hughes and Saudi Aramco Management for the permission to publish the results.

References

AhmadZamri, A.F., Musgrove, F.W., Bridle, I.M., Angelich, M.T. and vandenBosch, R. 2009. Successful Reservoir Monitoring with 4D Microgravity at Ras Laffan, State of Qatar. Paper IPTC 13640 presented at the 4th International Petroleum Technology Conference, Doha, Qatar, 7-9 December.

Alawiyah, S., Santoso, D., Kadir, W.G.A and Matsuoka, T. 2012. Time-lapse Microgravity Application for Estimating Fluid Density Changes of Multilayer Reservoir Using DSMVD Technique. Paper IPTC 14800 presented at the 5th International Petroleum Technology Conference, Bankok, Thailand, 7-9 February.

Alnes, H., Eiken, O. and Stenvold, T. 2008. Monitoring Gas Production and CO2 Injection at the Sleipner Field Using Time-lapse Gravimetry. *Article SEG Geophysics Journal,* November-December 2008 Issue, Vol. **73,** No.6, p. 155–161.

Alshakhs, M.J., Riis, E., Westerman, R., Lyngra, S. and Al-Otaibi, U.F. 2008. Utilizing 4D Microgravity To Monitor Water Encroachment. Paper SPE 115028 presented the 2008 SPE Annual Technical Conference and Exhibition, Denver, Colorado, USA, 21-24 September.

Al-Shehri, A.A., Ellis, E.S, Felix Servin, J.M., Kosynkin, D.V., Kanj, M.Y. and Schmidt, H.K. 2013. Illuminating the Reservoir: Magnetic NanoMappers. Paper SPE 164461 presented at SPE Middle East Oil and Gas Show and Conference, Manama, Bahrain, 10-13 March.

Ander, M. and Biegert, E. 2006. A New Approach to Subsurface Gravity. Expanded Abstract SEG-2006-0904 presented at the 2006 SEG International Exposition and 76th Annual Meeting, New Orleans, Louisiana, USA, 1-6 October.

Bate, D. 2005. 4D Reservoir Voumetrics: A Case Study over the Izaute Gas. *Article EAGE First Break Magazine* November 2005 Issue, Vol. **23,** p. 69–71.

Brady, J.L., Wolcott, D.S. and Aiken, C.L.V. 1993. Gravity Methods: Useful Techniques for Reservoir Surveillance. Paper SPE 26095 presented at the SPE Western Regional Meeting, Anchorage, Alaska, USA, 26-28 May.

Brady, J.L., Wolcott, D.S., Daggett, P.H., Ferguson, J.F., Hare, J.L., Aiken, C.L.V., Balde, M., Seibert, J.E. and Mader, G. 1995. Water Movement Surveillance with High Resolution Surface Gravity and GPS; A Model Study with Field Test Results. Paper SPE 30379 presented at the SPE Annual Technical Conference and Exhibition, Dallas, Texas, USA, 22-25 October.

Brady, J.L., Ferguson, J.F., Aiken, C.L.V., Seibert, J.E., Chen, T. and Hare, J.L 2002. Performing a High Resolution Surface Gravity Survey to Monitor the Gas Cap Water Injection Project, Prudhoe Bay, Alaska. Paper SPE 76740 presented at the SPE Western Regional / AAPG Pacific Section Joint Meeting, Anchorage, Alaska, USA, 20-22 May.

Brady, J.L., Ferguson, J.F., Seibert, J.E., Chen, T., Hare, J.L, Aiken, C.L.V., Klopping, F.J. and Brown, J.M. 2004. Surface Gravity Monitoring of the Gas Cap Water Injection Project, Prudhoe Bay, Alaska. *Article SPE 87662, SPE Reservoir Evaluation & Engineering Journal,* February 2004 Issue, Vol. **7,** No.1, p. 59–67.

Brady, J.L., Hare, J.L., Ferguson, J.F., Seibert, J.F, Klopping, F.J., Chen, T. and Niebauer, T.M. 2008. Results of the World's First 4D Microgravity Surveillance of a Waterflood - Prudhoe Bay, Alaska. *Article SPE 101762, SPE Reservoir Evaluation & Engineering Journal,* October 2008 Issue, Vol. **11,** No.5, p. 824–831.

Brown, J.M., Klopping, F.J., van Westrum, D., Niebauer, T.M., Billson, R., Brady, J.L., Ferguson, J.F., Chen, T. and Seibert, J.E. 2002. Preliminary Absolute Gravity Survey Results from Water Injection Monitoring Program at Prudhoe Bay. Expanded Abstract SEG-2002-0791 presented at the 2002 SEG International Exposition and 72nd Annual Meeting, Salt Lake City, Utah, USA, 6-11 October.

Chapin, D.A and Mann E.H. 1999. The Bold New World of Borehole Gravimetry. Expanded Abstracts SEG-1999-0393 presented at the 1999 SEG International Exposition and 69th Annual Meeting, Houston, Texas, USA, 31 October-5 November.

Dake, L.P. 2001. *The Practice of Reservoir Engineering* (Revised Edition). Textbook, Elsevier, ISBN 978-0-444-50671-9.

Davis, K., Kass, M.A., Krahenbuhl R. and Li, Y 2008. Survey Design and Model Appraisal based on Resolution Analysis for 4D Gravity Monitoring. Expanded Abstract SEG-2008-0731 presented at the 2008 SEG International Exposition and 78th Annual Meeting, Las Vegas, Nevada, USA, 9-14 November.

Eiken, O., Zumberge, M. and Sasagawa, G. 2000. Gravity Monitoring of Offshore Gas Reservoirs. Expanded Abstracts SEG-2000-0431 presented at the 2000 SEG International Exposition and 70th Annual Meeting, Calgary, Canada, 6-11 August.

Ferguson, J. F., Chen, T., Brady, J.L. Aiken, C.L.V. and Seibert, J.E 2007. The 4D Microgravity Method for Water Flood Surveillance: Part II - Gravity Measurements for the Prudhoe Bay Reservoir, Alaska. *Article SEG Geophysics Journal,* March 2007 Issue, Vol. **72,** No.2, p. 33–43.

Hadi, S., Alawiyah, S., and Kadir, W.G.A. 2013. Integration of 4D Microgravity, Geology and Production Data to Monitor Water Injection in Improved Oil Recovery Project, Diamond Field. Paper IPTC 17101 presented at the 6th International Petroleum Technology Conference, Bejing, China, 26-28 March.

Hadj-Sassi, K. and Donadille, J.-M. 2010. Three-Dimensional Inversion of Borehole Gravity Measurements for Reservoir Fluid Monitoring. Paper SPE 136928 presented at presented at the 2010 SPE/DGS Annual Technical Symposium and Exhibition, Al-Khobar, Saudi Arabia, 4-7 April.

Hare, J.L., Ferguson, J.F., Aiken, C.L.V. and Brady, J.L. 1999. 4-D Microgravity Modeling and Inversion for Waterflood Surveillance: A Model Study for the Prudhoe Bay Reservoir, Alaska. *Article SEG Geophysics Journal,* January-February 1999 Issue, Vol. **64,** No.1, p. 78–87.

Glegola, M., Ditmar, P., Hanea, R.G., Vossepoel, F.C., Arts, R. and Klees, R. 2012. Gravimetric Monitoring of Water Influx into a Gas Reservoir: A Numerical Study Based on the Ensemble Kalman Filter. *Article SPE 149578, SPE Journal* March 2012 Issue, Vol. **17,** No. 1, p. 163–176.

Glegola, M., Ditmar, P., Hanea, R.G., Eiken, O., Vossepoel, F.C., Arts, R. and Klees, R. 2012. History Matching Time-Lapse Surface Gravity and Well-Pressure Data with Ensemble Smoother for Estimating Gas Field Aquifer Support – A 3D Numerical Study. *Article SPE 161483, SPE Journal* December 2012 Issue, Vol. **17,** No.4, p. 966–980.

Judzis, A., Felder, R., Curry, D. and Seiller, B. 2011. The Five R&D Grand Challenges Plus One, Article 1 in R&D Grand Challenges - JPT Article Series. Paper SPE 163061. *SPE Journal of Petroleum Technology* May 2011 Issue, p. 34–35.

Jackson, D.D. 1979. The Use of A Priori Data to Resolve Non-uniqueness in Linear Inversion. *Article Geophysical Journal of the Royal Astronomical Society,* April 1979 Issue, Vol. **57,** No. 1, p. 137–158.

Krahenbuhl R. and Li Y.G. 2008. Joint Inversion of Surface and Borehole 4D Gravity Data for Continuous Characterization of Fluid Contact Movement. Expanded Abstracts SEG-2008-0726 presented at the 2008 SEG International Exposition and 78th Annual Meeting, Las Vegas, Nevada, USA, 9-14 November.

Krahenbuhl, R, Li, Y. and Davis, T. 2010. 4D Gravity Monitoring of Fluid Movement at Delhi Field, LA: A Feasibility Study with Seismic and Well Data. Expanded Abstracts SEG-2010-4210 presented at the 2010 SEG International Exposition and 80th Annual Meeting, Denver, Colorado, USA, 17-22 October.

Loermans, T. and Kelder, O. 2006. Intelligent Monitoring?. . .. Add Borehole Gravity Measurements! Paper SPE 99554 presented at the 2006 SPE Intelligent Energy Conference and Exhibition, Amsterdam, The Netherlands, 11-13 April.

Lyngra, S., Najjar, N.F. and Tsingas, C. 2013. Detection and Modeling of Natural Fractures: Real Life Detection Examples and Workflows for Implementing Fractures in Simulation Models. Extended astract EAGE-NFR35 presented at the 2nd EAGE Workshop on Naturally Fractured Reservoirs: Naturally Fracture Reservoirs in Real Life, Muscat, Oman, 8-11 December.

Marsala, A.F., Lyngra, S., Widjaja, D.R., Laota, A.S., Al-Otaibi, N.M., Zhanxiang, H., Zhao, G., Jiahua X. and Yang, C. 2013. Fluid Distribution Inter-Well Mapping in Multiple Reservoirs by Innovative Borehole-to-Surface Electromagnetic: Survey Design and Field Acquisition. Paper IPTC 17045 presented at the 6th International Petroleum Technology Conference, Bejing, China, 26-28 March.

Meyer T. 2010. Deep Diagonostics via Differential Microgravity Logging. Paper SPE 135036 presented the 2010 SPE Annual Technical Conference and Exhibition, Florence, Italy, 19-22 September.

Neal, J. and Krohn, C. 2012. Higher Resolution Subsurface Imaging, Article 5 in R&D Grand Challenges - JPT Article Series. Paper SPE 163061. *SPE Journal of Petroleum Technology* March 2012 Issue, p. 44–53.

Newton, I. 1687. *Philosophiæ Naturalis Prinicipia Mathematica*. The Royal Society of London for the Improvement of Natural Knowledge.

Van Nieuwenhuise, B. and Pramik, B. 2006. Resolution of Seismic, Gravity and Magnetic Data at Vertical Subsurface Interfaces Relevant to Seismic Imaging. Expanded Abstract SEG-2006-0889 presented at the 2006 SEG International Exposition and 76th Annual Meeting, New Orleans, Louisiana, USA, 1-6 October.

Peters, A., Chung, K.Y., Young, B., Hensley, J. and Chu, S. 1997. Precision Atom Interferometry. *Article, Philosophical Transactions of the Royal Society,* Vol. **355,** No. 1733, p. 2223–2233.

Santoso, D., Kadir, W.G.A., Sarkowi, M., Adriansyah and Walyuyo, W. 2004. Time-lapse Microgravity Study for Injection Water Monitoring of Talang Jimar Field. Paper presented at the 7th SEGJ International Symposium, Sendai, Japan, 24-26 November.

Tarantola, A. 2005. *Inverse Problem Theory and Methods for Model Parameter Estimation*. Textbook, Society for Industrial and Applied Mathematics (SIAM), ISBN 0-89871-572-5.

Zhdanov, M.S. 2002. *Geophysical Inverse Theory and Regularization Problems*. Textbook, Elsevier, ISBN 978-0-444-51089-1.